ADVANCED IMPREGNATED ACTIVATED CARBONS FOR FUEL CELL AIR PURIFICATION

A THESIS SUBMITTED FOR PARTIAL FULFILLMENT
OF THE REQUIREMENTS FOR THE DEGREE OF

BACHELOR OF SCIENCE

IN

GLOBAL ENVIRONMENTAL SCIENCE

December 2022

By

Jacob Vasquez

Thesis Advisor

Dr. Godwin Severa

I certify that I have read this thesis and that, in my opinion, it is satisfactory in scope and quality as a thesis for the degree of Bachelor of Science in Global Environmental Science.

THESIS ADVISOR

Godwin Severa
Hawai‘i Natural Energy Institute

For my family, friends, and all loved ones who have assisted and encouraged me in all my personal passions.

ACKNOWLEDGEMENTS

First and foremost, I would like to give a sincere appreciation to my mentor Dr. Severa for being such a fantastic mentor throughout this project in addition to his willingness to train and develop my skills in his laboratory. His knowledge and insight improved my perspective and approach for this project. This project would not be possible without his foresight, and I cannot express my gratitude to a greater degree. Additionally, I would like to thank Mr. Edward Bruffey III for his guidance and assistance throughout my training in the lab as well as execution of experiments.

I would also like to thank Mr. Keith Bethune for setting up the filtration stand and software, as well as always making himself available for whenever I had any issues or questions.

Lastly, I would like to thank my girlfriend and family for all their love and support throughout my college education and this project. Without their assistance I would not have been able to carry out this project from beginning to end.

ABSTRACT

Sulfur Dioxide (SO_2) emissions is continuing to be an escalating issue as the world relies on burning fossil fuels to produce electricity and support transportation. SO_2 can have severe health and environmental impacts, and is also capable of disrupting direct use of atmospheric air in emerging energy technologies. The focus of the project is to develop filter media with potential for the mitigation of SO_2 in proton exchange membrane (PEM) fuel cells. PEM fuel cells require filters to be able to remove air contaminants because the contaminants can poison the catalyst and/or damage the cells which reduce the power production, ultimately shutting down the entire system. The current state of the art methods of gas contaminant mitigation are mostly non-regenerable or are absorbing pollutants at low rates. Consequently, there is a need to develop alternate sorbent materials that are capable of higher performance and with regeneration capabilities.

To improve the current methods of air filtration technologies for SO_2, potential sorbent material were tested including; urea, tetramethylurea, melamine, boric acid, 1-ethyl-3-methylimidazolium acetate ([EMIM][OAc]), zinc 1-ethyl-3-methylimidazolium acetate (Zn[EMIM][OAc]), magnesium 1-ethyl-3-methylimidazolium acetate (Mg[EMIM][OAc]), manganese 1-ethyl-3-methylimidazolium acetate (Mn[EMIM][OAc]), potassium hydroxide (KOH). Impregnating these sorbents onto activated carbon and testing their performance under simulated harsh polluted air environments with flows of 1-2 LPM (5-15 ppm SO_2, clean air, 25˚C and 40-50% relative humidity) was performed. The results of gas sorption test showed that metallo ionic liquids presented improved filter media to some of the current industry sorbents.

Keywords: (gas-sorption, impregnation, filter-media, sulfur dioxide, breakthrough capacity, fuel-cell,)

TABLE OF CONTENTS

LIST OF TABLES

LIST OF FIGURES

1.0 INTRODUCTION

Air Pollution can have adverse effects to the human population, surrounding environment and exposed technologies. The impact on technologies requires innovative filter media to utilize absorbents and adsorbents to better protect technologies from contamination. For example, PEM fuel cells require filters to be able to remove contaminants because contaminants can poison the catalyst or damage the cells which reduce the power production, ultimately shutting down the entire system (Lv et al., 2022). The catalyst is an expensive and critical component of the fuel cell system, therefore it requires protection from contaminants. The current methods for preventing air contaminants from infiltrating the system and electrochemical reactions are unsatisfactory. They contribute to the short lifespans of fuel cell vehicles, as high flow rates and an increase of contaminants in the air contribute to the ineffectiveness of fuel cells after a non-competitive period of time (Lv et al., 2022). PEM fuel cell technologies can immensely benefit from the effective removal of acidic gas contaminants (e.g. SO_2 and H_2S) from air streams utilized as a cheap oxygen source for the fuel cell.

1.1 Air Pollution

Air pollution can originate from both anthropogenic and natural sources, but the most prominent pollution sources mostly come from the combustion of fossil fuels during energy production. A consequential impact of air pollution is the greenhouse effect. The greenhouse effect is the way heat is trapped to Earth's surface (Qiao et al., 2019). The greenhouse effect is trapping heat because the sun delivers shortwave radiation to the Earth and the Earth absorbs the shortwave radiation and re-emits longwave radiation. The emitted longwave radiation is unable to pass through the different greenhouse gases in the atmosphere and traps the heat to the Earth's surface (Stephens et al., 2012).

The leading contributing sources of greenhouse gases are transportation, electricity production, and industrial scale producers. Figure 1 displays these different sources of greenhouse gases. Transportation is a leading contributor because most transportation methods utilize combustion by burning fossil fuels (Shariat Panahi, 2019). Electricity production is a significant contributor to greenhouse gas emissions because approximately 60% of our electricity comes from the burning of fossil fuels, generally coal and natural gas. Additionally, significant contributions of greenhouse gas emissions are from burning fossil fuels for industrial usage. In addition to burning fossil fuels, industrial pollutants come from using particular chemical reactions to produce goods from raw materials (Shariat Panahi, 2019).

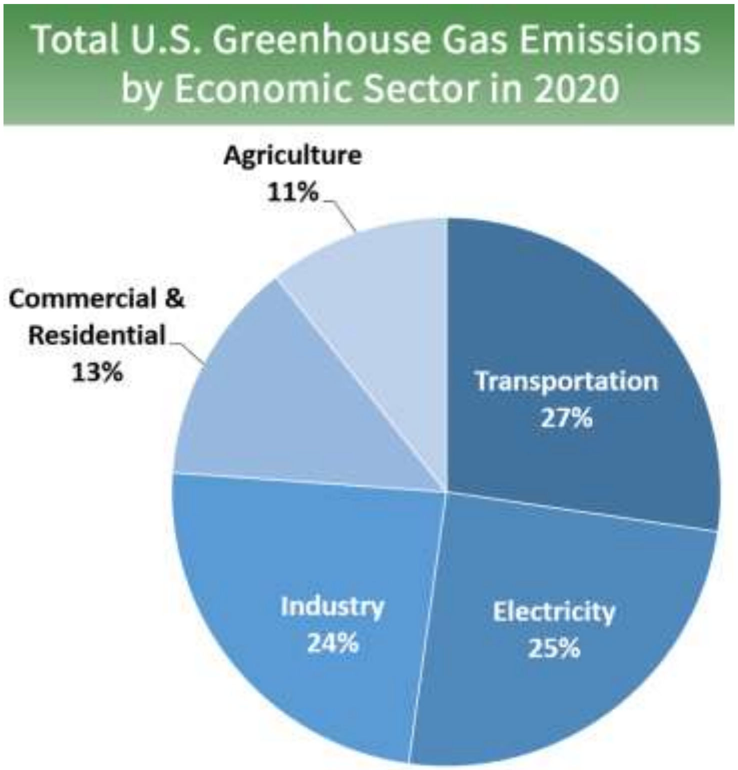

Figure 1: Sources of Greenhouse gases by economic sectors (Environmental Protection Agency) https://www.epa.gov/ghgemissions/sources-greenhouse-gas-emissions.

There are a variety of gases that are in the air and after being emitted bring upon different adverse effects to humans and the natural environment. A significant gas that has adverse effects is Sulfur dioxide-SO_2, other gases are redox forms of carbon (carbon dioxide-CO_2, carbon monoxide-CO, methane-CH_4) and nitrogen (nitrogen dioxide-NO_2, nitric oxide-NO, dinitrogen tetraoxide-N_2O_4, ammonia-NH_3, ammonium cation NH_4) (Khallaf, 2011). Other gaseous pollutants are benzene-C_6H_6, Ozone-O_3, mercury-Hg, volatile phenols, and Hydrogen Sulfide-H_2S (Khallaf, 2011). Table 1 exhibits different pollutants with corresponding emission sources, concentrations, and residence times.

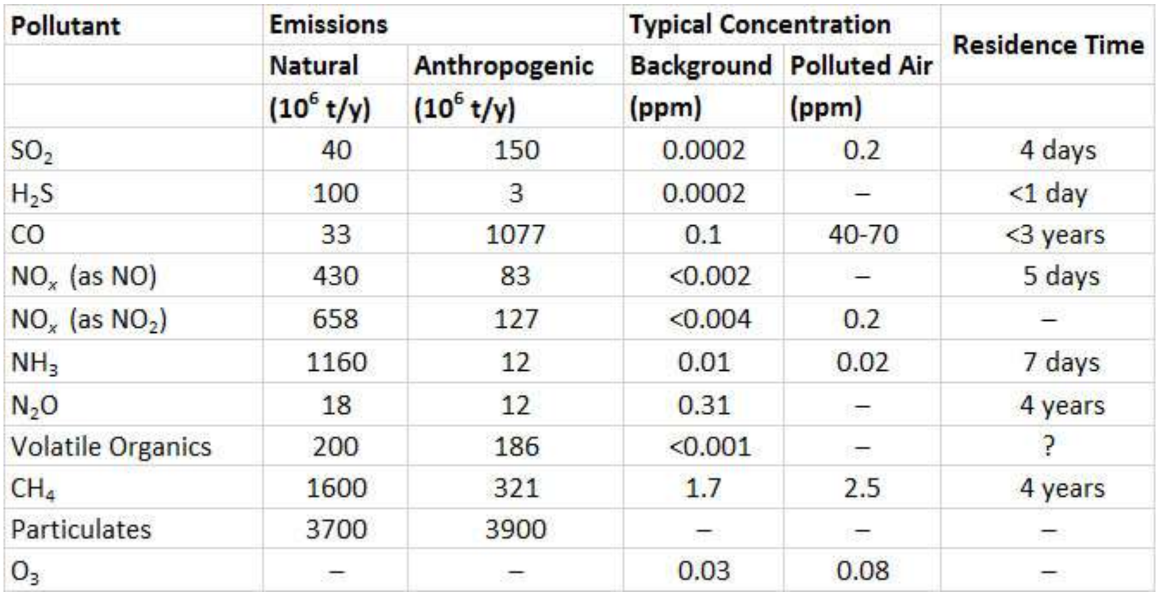

Pollutant	Emissions		Typical Concentration		Residence Time
	Natural	Anthropogenic	Background	Polluted Air	
	(10^6 t/y)	(10^6 t/y)	(ppm)	(ppm)	
SO_2	40	150	0.0002	0.2	4 days
H_2S	100	3	0.0002	–	<1 day
CO	33	1077	0.1	40-70	<3 years
NO_x (as NO)	430	83	<0.002	–	5 days
NO_x (as NO_2)	658	127	<0.004	0.2	–
NH_3	1160	12	0.01	0.02	7 days
N_2O	18	12	0.31	–	4 years
Volatile Organics	200	186	<0.001	–	?
CH_4	1600	321	1.7	2.5	4 years
Particulates	3700	3900	–	–	–
O_3	–	–	0.03	0.08	–

Table 1: Different Air Pollutants and their corresponding global emissions, as well as characteristics of the air pollutants. Source: Freedman (1995) and NEAA (2015). https://ecampusontario.pressbooks.pub/environmentalscience/chapter/chapter-16-gaseous-air-pollution/

An acidic gas responsible for significant environmental effects as well as health effects is SO_2. SO_2 is generally produced by burning fossil fuels but can also be emitted naturally by the eruption of volcanoes. SO_2 health impacts in humans who are exposed can include irritation of the eyes, but most impacts are within the respiratory system, more specifically the lungs (Aguilar-Dodier, 2020). SO_2 irritates the respiratory tract and can influence tract infections. Typically, symptoms are coughing and mucus secretion, but can also severely aggravate conditions such as asthma and chronic bronchitis (Aguilar-Dodier, 2020; Queensland, 2017).

Another acidic gas that can have harmful impact is CO_2, and CO_2 is a particularly dangerous pollutant because of its long lifespan in the atmosphere and significant contribution to the greenhouse effect. CO_2 is emitted into the atmosphere through two different ways; burning fossil fuels and volcanic eruptions (Eufrasio et al., 2022). CO_2 is minimally toxic by inhalation; the primary health impact from inhaling CO_2 is that CO_2 reduces or displaces normal oxygen in breathing air. Mild CO_2 inhalation symptoms can include headaches and drowsiness, but more severe exposure can cause rapid breathing, confusion, increased cardiac output, elevated blood pressure, and increased arrhythmias (Eufrasio et al., 2022). CO_2 also plays a significant role in global warming and climate change because of intensifying the greenhouse effect (Eufrasio et al., 2022).

The next important acidic gas to cover is NO_2 which is a toxic gas that can have significant repercussions on public health. NO_2 is typically formed in the atmosphere by reactions of NO and ozone, but there are also NO_2 emissions from transportation. Diesel fueled vehicles in particular typically contribute the more significant amounts of NO_2 emissions in regard to transportation (Carlsaw and Beevers, 2004). NO_2 in high concentrations can have a severe impact on human health. Exposure to NO_2 causes inflammation of the airways and cardiovascular disease (WHO, 2013; Latza et al., 2009). When exposed to more severe concentrations of NO_2, the health impacts can even cause morbidity and mortality. In a 2016 European Environmental Agency report, NO_2 was responsible for 71,000 premature deaths in Europe, and is also a contributing factor for about 2 million asthma cases among children worldwide (EEA, 2016; Butera, 2022). In addition to the direct health impacts from NO_2, the acidic gas NO_2 is also a major concern as it contributes to the generation of secondary aerosols and tropospheric ozone in the atmosphere, which have additional impacts on human health and the environment (Finlayson-Pitts and Pitts, 2000).

H_2S is another gas that has significant environmental and health impacts. H_2S is released into the atmosphere in both natural and unnatural processes. The harmful gas can be released by crude petroleum, natural gas, volcanic gases, liquid manure, sewage, sludge, landfills, and sulfur hot springs (VDH, 2021). H_2S has health impacts that can be evident in asthmatics. Exposure to H_2S may cause irritation to the eyes, and higher concentrations of H_2S causes irritation to the upper respiratory tract. At significantly high concentrations, which are roughly 150ppm, hydrogen sulfide can paralyze the olfactory nerve, and when concentrations reach 200 to 300 ppm, H_2S effects can become life-threatening (Aguilar-Dodier, 2020; VDH,2021). H_2S emissions are capable of forming SO_2 and sulfuric acid when emitted into the atmosphere, which has additional health and environmental impacts (Aguilar-Dodier, 2020; VDH,2021).

Particulate matter is another form of air pollution and can present detrimental health impacts because of its small size. Particulate matter emissions are from direct sources such as construction sites, unpaved roads, fields, smokestacks, and/or fires (EPA, 2021). Particulate matter can pose severe health problems, and, the smaller the size, the more severe the health problems are that arise. Smaller particles can go deep into the lungs and sometimes into the bloodstream, where the particles can impact both the lungs and heart. These particles have been linked to premature death in people with heart or lung disease, nonfatal heart attacks, irregular heartbeat, aggravated asthma, decreased lung function, and increased respiratory symptoms (EPA, 2021). Particulate matter can also have environmental effects. Particulate matter is capable of impairing visibility, making lakes and streams more acidic, shifting the nutrient balance in coastal waters and large river basins, depleting nutrients in soil, damaging sensitive forest and farm crops, impacting the diversification of ecosystems, and contributing to acid rain effects (EPA, 2021).

Overall, air pollution can have severe repercussions to human health. These health impacts can be separated into both acute (short term) and chronic (long-term) exposure. Acute exposure to air pollutants can cause individuals to be vulnerable to respiratory diseases, coughing, shortness of breath, wheezing, and Chronic Obstructive Pulmonary Disease (World Health Organization, 2021). The chronic effects that can be connected to air pollution are chronic asthma, pulmonary insufficiency, cardiovascular diseases, and cardiovascular mortality (World Health Organization, 2021).

Air pollution can also have adverse impacts on the environment where it is located. For instance, air pollution is the principal factor contaminating water vapor to generate acid rain. Acid rain is precipitation carrying harmful amounts of nitric and sulfuric acids (Grennfelt, 2020). This harmful precipitation can damage trees, acidify bodies of water and soil, and create an unsuitable environment for some fish and other wildlife. Lastly, a significant impact that air pollution can bring to the environment is climate change. Through the greenhouse effect, air pollution is causing the Earth's average temperature to rise and is causing detrimental climatic events across the globe (Grennfelt, 2020).

1.2 Current Absorbents and Adsorbents

The current industrial control methods to deal with acidic gases include flue gas desulfurization, dry sorbent injection, and dry sorbent injection with a fabric filter. Flue gas desulfurization is the installation of technologies to capture SO_2 from post-combustion waste gases (Institute of Clean Air Companies, 2016). The dry sorbent injection method is the injection of dry alkaline minerals into a flue gas stream in order to reduce acid gas emissions. The dry sorbent injection approach to removing acid gas emissions is recognized as an inexpensive solution and is growing to be a popular alternative to the other absorption technologies (Institute of Clean Air Companies, 2016). Dry sorbent injection methods allow for a broad range of operation. This will allow efficient use of the reagent even with load changes, fuel changes, and operational cycling (Institute of Clean Air Companies, 2016). A fabric filter is an apparatus that separates and accumulates particulate matter from flue gas streams. To be able to optimize the amount of particulate loading from the flue gas streams, a fabric filter could be used with dry sorbent injection (Institute of Clean Air Companies, 2016).

Ionic liquids have significant potential for gas sorption; ionic liquids have desirable characteristics such as being non-volatile and having high gas pollutant sorption kinetics (seen in Figure 2). Therefore, ionic liquids play an important role in gas sorption. [EMIM][OAc] was successful in SO_2 capture when impregnated onto activated carbon (Severa et. al, 2015). Other forms of adsorbents and absorbents that were tested in this project were Zn[EMIM][OAc], Mg[EMIM][OAc], Mn[EMIM][OAc], urea, tetramethylurea, boric acid, melamine, and KOH. These were all tested because of their tunable structure characteristics that make them suitable options for gas sorption.

1.3 Supports

Activated carbons are utilized for numerous filtration applications including as adsorbents, catalyst supports, and in gas separation. In the filtration industry, activated carbon plays a critical role in environmental protection of pollution control which includes removal of gases such as SO_2 (Bandosz, 1999). Activated carbon is successful for adsorption because it is a highly porous material and possesses a high surface area that leaves room for the contaminate gases to absorb into (Severa et. al, 2015). The characteristics of activated carbon also makes a prominent candidate for a support to impregnate sorbents onto the surface. Using activated carbon as a support and impregnating the various sorbents can increase the potential for acidic gas sorption (Severa et. al, 2015).

1.4 Fuel Cell Application

Climate change is increasingly gaining attention in the political sector, encouraging scientists, engineers, and policy makers to improve and convert the current contributors to greenhouse gas emissions and other sources of the issue and create new sustainable alternatives. A significant contribution to climate change comes from transportation. Most transportation methods are predominantly using petroleum as their main source for combustion to power vehicles (Colella et. al, 2005). Another issue is that individuals are generally not using mass transportation and instead using personal vehicles. The use of individual transportation methods is intensifying the issue, and with an exponentially growing population, this rate of unsustainable transportation cannot continue. This trend demands new, innovative ways to adapt and create transportation methods that will not contribute harmful greenhouse gases to the atmosphere, while being desirable enough to make a realistically competitive alternative in the market.

One such possible adaptation in the current transportation system is the use of electric/hybrid vehicles powered by hydrogen using PEM fuel cells. PEM fuel cells are an applicable alternative and competitive option, currently ranking in highest reduction of greenhouse gas emissions with the highest amount of energy output among vehicular transportation options (He et.al, 2021). Fuel cells do not produce power through combustion but instead through an electrochemical reaction. A fuel cell is a device that utilizes hydrogen and oxygen to generate electricity and has byproducts of water and heat. The fuel cell system does this by having hydrogen atoms enter at the anode (negative electrode that releases electrons) where the atoms are stripped of their electrons (Haile, 2003). On the other side of the fuel cell system, the positively charged protons will pass through the membrane to the cathode (positive oxidizing electrode that receives the electrons) and the negatively charged electrons are forced through a circuit, generating electricity. After going through this circuit, the electrons combine with the protons and oxygen from the air to generate the byproducts of the fuel cell; water and heat (Haile, 2003).

A major challenge in PEM fuel cells that is necessary to address is the durability of their vehicles. The issue of durability is difficult to tackle because the use of fuel cells needs to be able to operate in a vastly wide range of conditions. As of 2020, fuel cell durability was around a third of what it needed to be to become competitive. The durability was projected for fuel cell vehicles to last around 57,000 miles, but the goal lifetime for fuel cell vehicles is 150,000 miles to compete with the conventional combustion vehicle

(Office of Energy Efficiency & Renewable Energy, 2020). Another issue with the durability of fuel cell vehicles is that their systems always contain water, and if these vehicles are operating in extreme cold weather this water can freeze. If the water in the fuel cells freezes, this would disrupt the entire electrochemical reaction and stop the vehicle (Office of Energy Efficiency & Renewable Energy, 2020). The other factor of the durability of fuel cells is that part of the system is taking in outside air for the O_2 part of the electrochemical reaction, opening a possibility for the air entering the fuel cell to be contaminated. These contaminants can hurt the performance of the fuel cell as well as shorten the life span of the fuel cell (Office of Energy Efficiency & Renewable Energy, 2020).

For fuel cells to be a competitive option there needs to be more development in materials that can filter the contaminants in the intake air more efficiently and in a more cost-effective method. The contaminants that are hurting the performance of fuel cells are particulate pollutants and gas pollutants. The particulate pollutants include ash, dust, metallic (Hg etc.), and nonmetallic (sulfates, nitrates, etc.) compounds. The gas pollutants are sulfur oxides, nitrogen oxides, carbon oxides, volatile organic compounds, and ground-level ozone (Cheng et al., 2006). The current approaches to remove these pollutants and protect the integrity of the fuel cell system primarily consist of two methods, one being pure activated carbons. The other current method for filtering out these contaminants from entering the fuel cell system is impregnated activated carbons and impregnated silica. Common choices for impregnation with activated carbon include ionic liquids, but other possibilities are metal hydroxides, metal oxides, and metals (Freudenberg, 2020). The current disadvantage of these two approaches is that both will create substantial waste, and this waste could be hazardous to the environment because it has absorbed acidic gases and has used different compounds that consist of hazardous properties (Cheng et al., 2006). A possible solution is for filter media to be created for regenerative capabilities to be able to recycle the sorbents.

1.5 Metallo Ionic Liquid Potential for SO_2 Filter Media

When choosing sorbents to impregnate onto the activated carbon, the project looked to previously synthesized materials that presented desirable characteristics for SO_2 sorption. Traditional ionic liquids indicated effective interactions with SO_2 and NO_2 with acetate groups. The interaction between acetate groups and acidic gases is demonstrated in Figure 2 where SO_2 and NO_2 bonded with the acetate groups of ionic liquids (Severa et al., 2018). This led to the design and synthesis of novel metallo ionic liquids to be characterized and evaluated for SO_2 sorption capabilities. The metallo ionic liquid synthesized was $Mn_4(OAC)_{10}[C_2mim]_2$ and crystallization was performed as seen in Figure 3 (Dera et al., 2020). In the crystallization images, the structure contained a high content of acetate groups and large voids. The large voids and high content of acetate groups proposed significant opportunities for acidic gas capture.

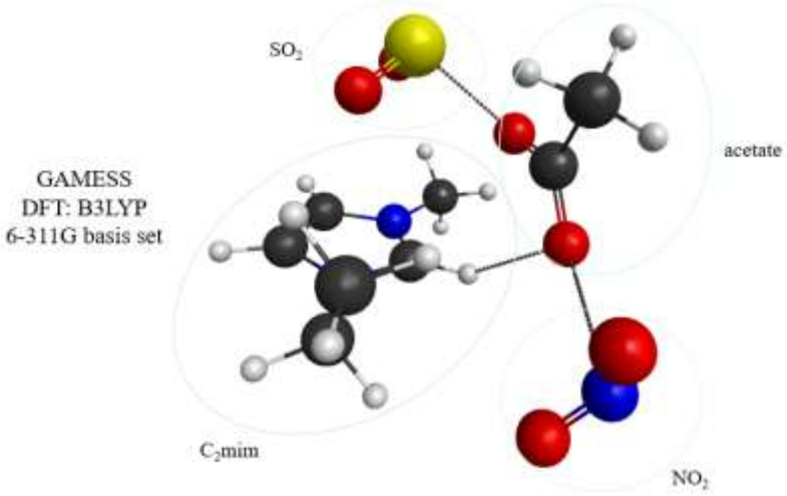

Figure 2. Ionic Liquid binding capabilities to SO_2 and NO_2.

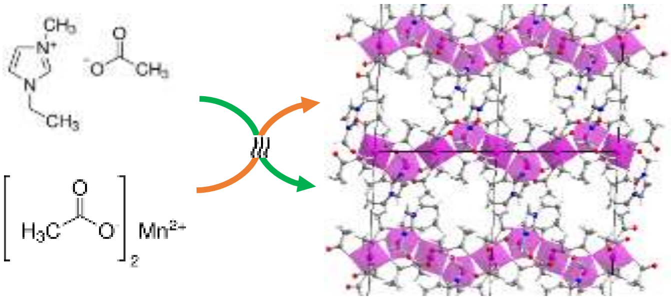

Figure 3. Crystal structure of the novel $Mn_4(OAc)_{10}[C_2mim]_2$ compound.

2.0 METHODS

To test the performance levels of different impregnated sorbents, the initial step that is required is washing and drying the activated carbon. After thoroughly washing the activated carbon, incipient impregnation of the sorbent onto the activated carbon can be performed. Lastly the newly created sorbent is ready to be tested for acidic gas capture and be evaluated as an effective or non-effective sorbent.

2.1 Preparation of Activated Carbon

The project used Norit GCN 830 activated carbon. The Norit GCN 830 activated carbon needed to be washed and dried to have a more successful impregnation. Washing and drying of the activated carbon was to remove any powder from the pores. The process started by taking the activated carbon, pouring it into a beaker, and then filling the beaker with sink water and stirring with long stirring tool. The water was then drained out into a separate container that had a cloth filter to catch any activated carbon. The captured activated carbon was then placed back into the first container. This process was repeated until the filtered water was clear and less murky. The process took approximately 5– 6 times using sink water. Then the activated carbon was washed using deionized water and was repeated until the filter water was clear which took another 5-6 times. Next as much of the water as possible was taken out of the washed activated carbon beaker and the activated carbon was poured onto a cloth and sat for approximately 1 hour to let any water flush out. The activated carbon was then placed into the vacuum oven and dried at 105˚C for 48 hours, or until there was no condensation occurring on the oven glass to indicate the activated carbon was completely dried. See Appendix 1 to see an outlined procedure on how to wash and dry the activated carbon.

2.2 Incipient Impregnation

When creating the [EMIM][OAc] 10% and 30% impregnated activated carbon, the materials used [EMIM][OAc] and methanol (solvent) were prepared using the incipient impregnation method at 25˚C. Appendix 2 table outlines the general procedure for impregnating the sorbent onto the activated carbon. To prepare the sorbents, 2.22g and 8.57g of [EMIM][OAc] were weighed out into two separate 125mL flasks. It was important when dropping the ionic liquid into the flask to avoid any ionic liquid contacting the sides of the flask. If any ionic liquid had contact with the sides of the flask, the ionic liquid's viscous nature would cause it to stick to the side and make it more difficult for a full reaction. If any ionic liquid was stuck to the sides of the flask, a solvent was utilized by pipetting the solvent onto the sides to help mix and push down the viscous ionic liquid from the sides to the bottom. The ionic liquid was then mixed with methanol; the 2.22 g [EMIM][OAc] 10% solution was mixed with 8.28 mL of methanol, and the 8.57 g [EMIM][OAc] 30% solution was mixed with 2.5 mL of methanol.

Two 20-gram samples of washed/dried activated carbon were prepared and sealed with parafilm to keep any water from sorbing into the activated carbon until the experiment was ready to take place. The activated carbon was then poured into the ionic liquid solutions and agitated directly using a vortex mixer, shown in Figure 4. The sample is placed on the center of the vortex mixer and was initially mixed for short periods of time, 5 seconds on and 5 seconds off. When the sample was taken off the vortex mixer, the sample was agitated by hand to try to mix the activated carbon up and push down any activated carbon that was stuck to the sides. After a few intervals of the short placement periods, the sample was placed on the vortex mixer for longer periods of time, approximately 10 seconds on and 10 seconds off. Any activated carbon that was remaining on the sides was continually agitated down when taking the sample off the mixer. During the process, the bottom of the flask was continuing to be observed for heat, because the reaction was exothermic and released heat. The heat provided an indication of how much longer the sample should be agitated on the vortex mixer. After mixing at longer periods, the agitation periods returned to short periods of 5 seconds on and 5 seconds off. Once there was no longer any liquid or activated carbon appearing to be on the glass, the samples were left for approximately 20 hours at 25˚C with occasional agitation. Next, samples were placed into the vacuum oven for 20 hours at 105 ˚C to remove the methanol. The samples were then stored in an inert glovebox.

Figure 4: Vortex mixer aiding in agitation of sorbent onto activated carbon support. In the picture this particular impregnation was the Manganese [EMIM][OAc] sample.

In a third flask 2.05 g of potassium hydroxide was measured out and dissolved in 8.9 mL of water. Then 18 grams of activated carbon was measured and mixed into the KOH solution. The process of agitating was the same as the agitation process for [EMIM][OAc]. Once the KOH sample was finished with agitation the sample sat for 20 hours at room temperature with occasional agitation. The newly created sample was dried in a vacuum oven (Below in Figure 5) for 20 hours at 105 ˚C to pull off the water solute of the KOH impregnated activated carbon.

Figure 5: The vacuum oven is the equipment on the stand. The evacuation is operated through the pump located on bottom left (blue equipment).

The following sorbents were incipient impregnated in smaller concentrations, as these were the new sorbents that had never been tested using this method before. These sorbents included urea, tetramethylurea, melamine, boric acid, Zn[EMIM][OAc], and Mg[EMIM][OAc] and Mn[EMIM][OAc]. These sorbents were impregnated onto 5.0 g of activated carbon and various concentrations depending on their solubility.

The first of the new sorbents was urea and was measured out at 1.1 g (Table 2) and dissolved in water using a 5 mL volumetric flask. The 1.10 g of urea was first funneled into the volumetric glass and then water was added as a solute to the urea and filled for a total volume of 5 mL. Using a previously made calculation on the total volume of the pores of the activated carbon, it was known that the total volume of the pores was 50% of the volume of activated carbon. The total pore volume of activated carbon was 2.5 mL, so the sorbent solution should have been 2.5 mL to fully fill the pores . This led to the reasoning of the next step of extracting 2.5 mL out of the 5 mL volumetric flask and pouring it into a 125 mL flask, again avoiding contacting the sides of the flask. The 5.0 g of the activated carbon was then poured into the urea water solution and was agitated immediately using a vortex mixer, the same as KOH and [EMIM][OAc] stated previously. Once the urea sample was finished, the sample sat for 20 hours sitting in room temperature with occasional agitation. The newly created solution was dried for 5 hours at 105 ˚C to pull off the water solute on the urea impregnated activated carbon.

The remaining samples followed the process of using a 5 mL volumetric flask for solubility, agitation with the vortex mixer, then dried in the vacuum oven for 5 hours. The only key difference for the remaining sorbents were the weight percentages because of solubility reasons. These weight percentages and exact sorbent/solvent information can be seen in Table 2 below.

Absorbent	Absorbent Amount	Activated carbon (g)	Solvent	Total volume (ml)	Estimated wt %	Mixture Extracted (ml)
Urea	1.130 g	5	Water	5	10.15	2.50
Melamine	0.152 g	5	Water	5	1.50	2.50
KOH	2.050 g	18	Water	9	10.22	na
EMIM 10%	2.220 g	20	Methanol	10	9.99	na
EMIM 30%	8.570 g	20	Methanol	10	30.00	na
Tetramethylurea 10%	1.165 ml	5	Water	5	10.43	2.50
Tetramethylurea 30%	4.440 ml	5	Water	5	30.75	2.50
Boric Acid	1.224 g	5	Methanol	5	10.90	2.50
Zn[EMIM][OAc]	0.565 g	5	Water	5	5.35	2.50
Mg[EMIM][OAc]	1.100 g	5	Water	5	9.91	2.50
Manganese [EMIM][OAc]	0.565 g	5	Methanol	5	5.35	2.50
Zn[EMIM][OAc]	0.429 g	2	Water & Methanol	2	9.69	1.00

Table 2: List of sorbents impregnated onto activated carbon with corresponding weight percentages and solvents used.

Table 2 above presents the other sorbents that were incipient impregnated onto activated carbon. Sorbents that could reach 10% concentration given strong solubility were tetramethylurea (water), Mg[EMIM][OAc] (water), and Zn[EMIM][OAc] (methanol). Tetramethylurea, being already in a liquid state, had high solubility and could reach 30%. Others that had lower or unknown solubility were melamine having a 1.5% concentration, Mn[EMIM][OAc] with a 5% concentration using methanol, and Zn[EMIM][OAc] with a 5% concentration using water as a solvent. All were still agitated and placed on the vortex mixer in the same manner as the urea sample, and then dried under vacuum for the same time of 5 hours at 105 ˚C. All impregnated samples were stored in the inert glovebox to avoid any water sorption.

2.3 Gas Analyzers

The system that analyzed the inlet concentrations of the acidic gas and the outlet concentration gases was an Enmet GSM-60 Fixed Gas Detection System. This unit used electrochemical sensors to determine concentrations of acidic gases. These sensors required calibration whenever replaced as well as every 3 months to ensure accuracy of the system. When calibrating the SO_2 electrochemical sensor, the calibration used the same conditions as if running a sorption experiment. These conditions were setting the heater to 25 ˚C, 13.8 ˚C dew point, a total flow rate of 2 Liters/minute (LPM), a flow rate of 0.5 LPM to the first inlet sensor, and a 1.5 LPM to the outlet sensor. For the 10 ppm calibration, clean air was used from a Matheson Ultra Zero Air cylinder containing 20-22% Oxygen, < 1ppm of CO_2, < 1ppm CO, < 0.1ppm of THC, and < 2ppm of H_2O. The 10 ppm calibration in combination with using the clean air gas used an air gas bottle of SO_2 of a concentration of 188.7pmm SO_2. The flow rates to make 10 ppm with a 13.8 ˚C dew point was 1.9 LPM of clean air and 0.1 LPM of impurity gas (SO_2).

The system needed to be running for approximately 25 minutes with all of the conditions set to reach the desired 13.8 ˚C dew point. After the system reached dew, the calibration was carried out. The calibration that the GSM-60 used was a two-point calibration; the first point being a zero concentration of impurity gas and the second point being the desired concentration at the high end of the measurement range of the sensor. The calibration method was already built into the GSM-60 units as a system maintenance menu. In the window, the first point of the calibration was inputted. This first point was only flowing the clean air at 2 LPM and not flowing the impurity gas at all to reach the zero concentration. In the system maintenance window, an electrometer in the display showed when the system was stable by seeing the number stabilize and change less frequently, then the system was stable enough to accept the calibration. After accepting the first calibration, the flow rates were changed to the corresponding flow rates for the 10ppm concentration, which was 1.9 LPM of clean air and 0.1 LPM of SO_2. Then the system took a few minutes to stabilize and then once the concentration was stable at 10 ppm and was ready to accept the calibration, the system automatically calculated the slope and offset values for calibration and then the GSM-60 was calibrated and ready for utilization.

2.4 Gas Sorption Experiments

Gas sorption experiments were conducted using a custom filtration stand shown in Figure 6. This filtration stand utilized two GSM-60 (gas monitoring) units, a humidifier, a heater, four mass flow controllers, and was tethered to a computer with custom-designed software to place conditional inputs and export graph outputs. The entire system was connected to two clean air gas cylinders and 3 acidic (impurity) gas cylinders (NO_2, H_2S, and SO_2) shown in Figure 7. The next steps were utilizing the software and filtration stand to choose which impurity cylinder to flow to the reactor, control flow rates for impurity and clean air gases, and direct the gases to the reactor where the sample was placed or bypassing the reactor to have gases go straight to the sensors without any interaction of the sample. Appendix 3 table displays the general method for performing gas sorption with the samples.

Figure 6: Custom filtration stand with two GSM-60 units on top of stand with software installed on laptop (right-side)

The first thing to determine for the sorption of SO_2 was the amount of each sample to use. Given the sorption capabilities of activated carbon with acidic gases, the sample size needed to have a short breakthrough time for experiments to have the best timeframe and to be efficient with the gas cylinders available. Different sizes ranging from 0.20 grams to 1.0 grams were tested to find the best time frame. The conditions set were the same as SO_2 sorption on the impregnated samples. The conditions were a 1.5 LPM flow rate into the reactor, 40%-50% relative humidity, and ~28 ˚C temperature. The activated carbon that was used as samples for screening sizes was the washed and dried activated carbon that was discussed in section 2.1 methods section. The samples were then placed into the reactor and the length of the sample in the reactor was measured and recorded. The gas cylinders and flow rates were already set, and the experiment began; see Figure 9 in results section.

To be able to accurately assess the gas sorption capabilities of the newly impregnated materials, it was necessary to have a baseline of data for pure activated carbon. The baseline sorption experiments were conducted multiple times. There were experiments using old sensors as well as experiments using new sensors. The old sensors were expired so the specific time data for the breakthrough capacities was not accurate, but the trends in the old sensor data stayed consistent and served as prominent preliminary data for screenings of activated carbons. In Figure 10 and Figure 11, the data displays gas sorption testing of pure activated carbon with 10 ppm of SO_2 gas being flowed through the sample.

The electrochemical sensors in our gas detection units were installed prior to the beginning of this project, and replacement sensors were ordered to make sure data was accurate. There were experiments ran with both the old sensors and the new sensors. Although the old sensors were calibrated, they were more saturated and contained more error. But were still able to provide sufficient results and served an excellent purpose of testing most of the sorbents and presented the successful sorbents.

After determining the activated carbon size and finding the breakthrough trends of the 0.25g AC, the impregnated sorbents were then tested. The flow rates were the same as both the testing of pure activated carbon and electrochemical sensor calibration. The flow rate of the clean air cylinder was set at 1.9 LPM, the SO_2 cylinder set at 0.1 LPM. The temperature was room temperature which was roughly ~28 ˚C, and the adjusted the humidifier to obtain a dewpoint of 13.8 ˚C. After the determined conditions were satisfied the gas was flowed into the reactor where the 0.25 g impregnated material was placed, and then the experiment began. The experiment timeframes changed depending on their success in sorption of SO_2. Typical experiments ran from 2 hours to 6 hours.

For this project the sorbents being tested were mostly new and their SO_2 sorption capabilities were unknown, so the first phase of the project was a screen testing for all of the newly tested sorbents to identify what sorbents were successful at SO_2 sorption.

Figure 7: All gas cylinders used for this project from left to right: SO_2 concentration 188.7ppm, NO_2 concentration 200.7 ppm, H2S concentration 200 ppm, and the last two are the Ultra-Zero Clean Air.

Figure 8: Polystat humidifier which was filled with deionized water to control relative humidity and dewpoint for the space in the reactor.

3.0 RESULTS

3.1 Baseline Activated Carbon Sorption

To determine the best sample size to test for all the SO_2 sorption testing experiments, a range of different activated carbon sample sizes were tested. The screening of different activated carbon sizes was tested at the same experimental conditions of 1.9 LPM of clean air, 0.1 LPM SO_2, room temperature ~ 28 ˚C, dew point of 13.8 ˚C, flow to inlet sensors 0.5 LPM and flow to reactor of 1.5 LPM. The range in sample sizes for the screening experiments was 0.2 g up to 1.0 g. In Figure 9 the graph shows the normalization of outlet concentrations divided by inlet concentrations represented as the C/C_0 value on the y-axis. This is in order to identify breakthrough capacities, and, for this screening, to select what sample size can be used for future examples that has a reasonable timeframe.

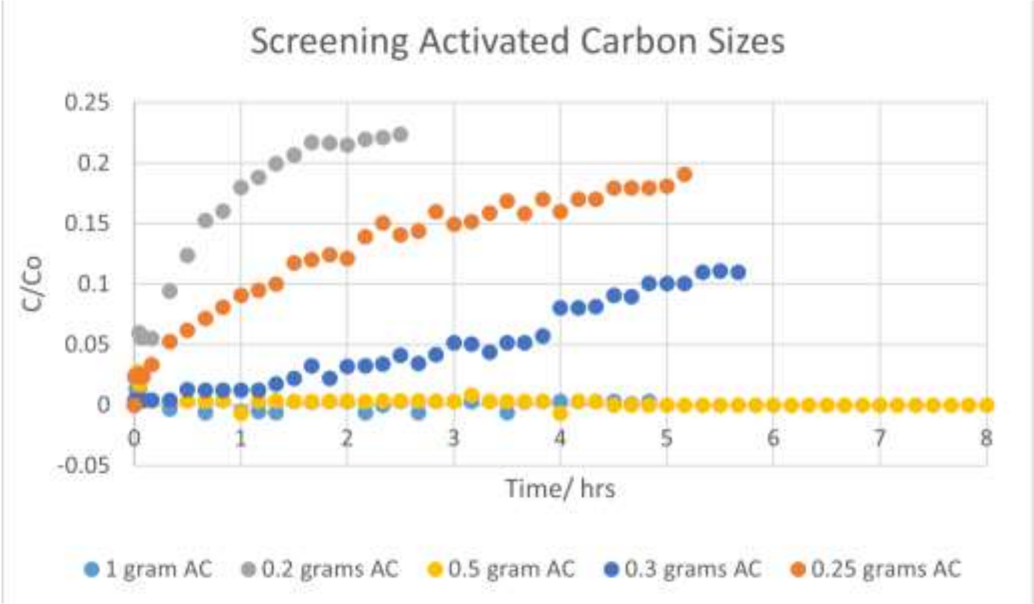

Figure 9: Figure showing normalization of concentrations in inlet sensor (~10ppm) divided by outlet sensor concentrations, showing when there is a breakthrough of SO_2 in activated carbon sample sizes ranging 0.2 g to 1.0 g.

The size of the sample to be placed into the reactor was determined, and the next step is to test the pure activated carbon for breakthrough capacity. .Before moving onto the SO_2 gas sorption, it was necessary to identify the breakthrough capacity trends of the pure activated carbon to identify what SO_2 sorption capabilities pure activated carbon presented and to be able to distinguish improvements in further sorption testing with the impregnated samples. The results shown in Figure 10 & Figure 11 demonstrate a breakthrough at approximately 10 minutes with the old sensors and a breakthrough at approximately 35 minutes with the new sensors. This data is now available to be included in the graphs showing results of impregnated materials.

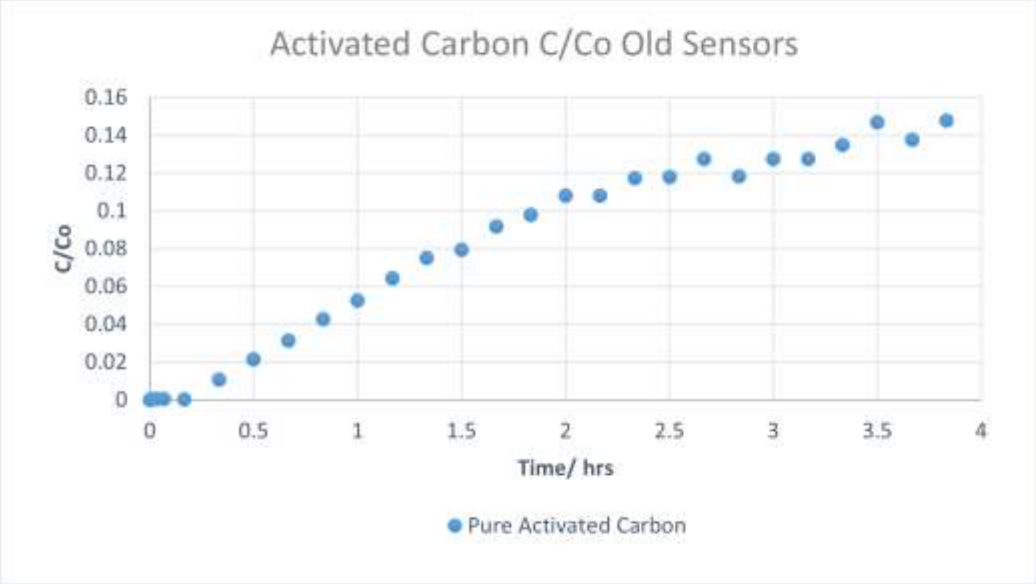

Figure 10: Activated carbon concentration of inlet (~10ppm) divided by outlet concentration, showing when there is a breakthrough of SO_2 in the old sensors.

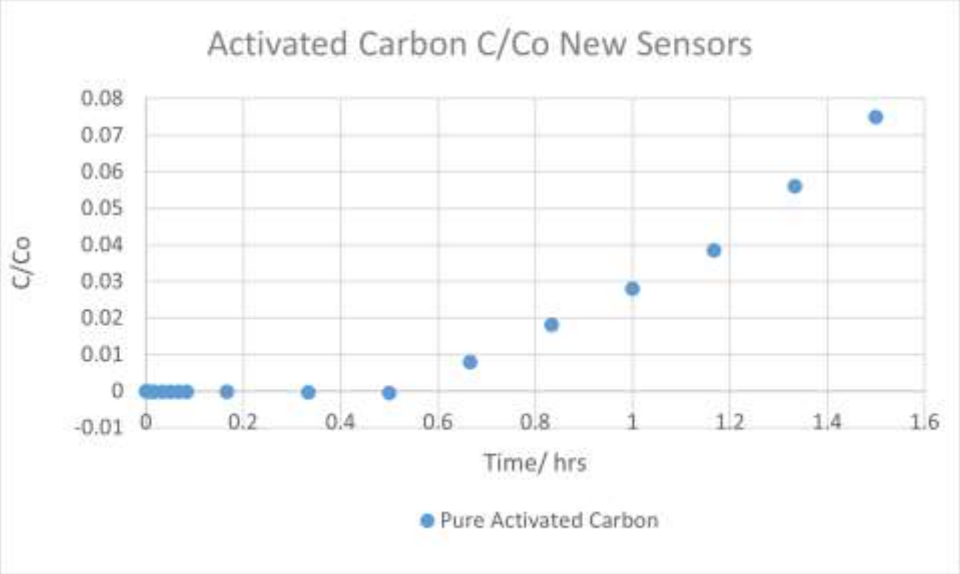

Figure 11: Activated carbon concentration of inlet (~10ppm) divided by outlet concentration, showing when there is a breakthrough of SO_2 in the new sensors.

3.2 Sulfur Dioxide Sorption Screening Tests

The SO_2 sorption also stayed within the same conditions that were set in the 3.1 baseline activated carbon sorption. In Figure 10 the graph displays the sorbents that were tested under a normalization scatter plot. The new unknown sorbents that hadn't been tested in these experimental atmospheric conditions are urea, tetramethylurea, and melamine. Potassium hydroxide was used as a comparison to industry standard, and to identify any improvement with new sorbents to some of the filter media used in industry.

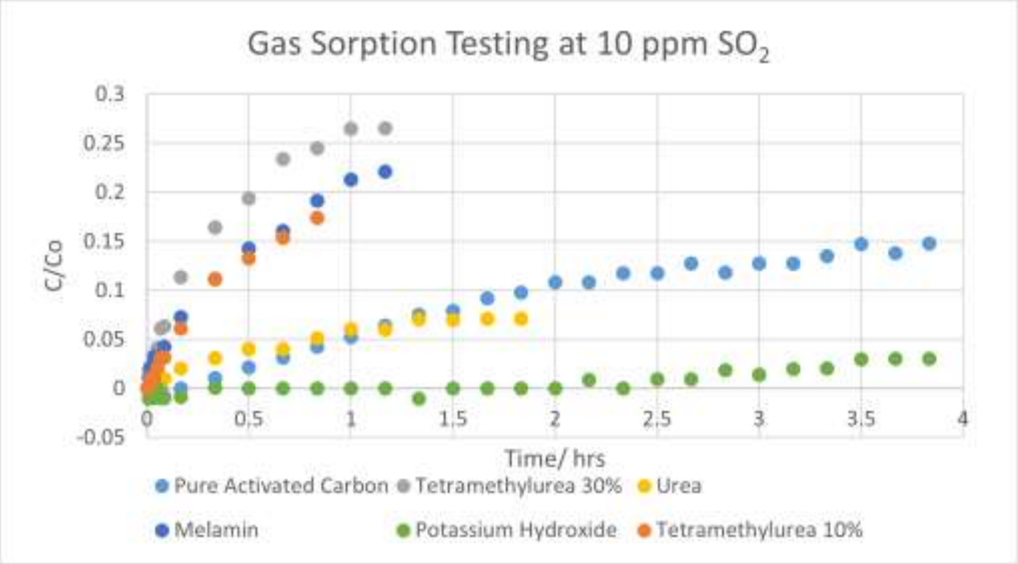

Figure 12: Impregnated activated carbon tested for 10 ppm SO_2 capture under realistic atmospheric conditions using a sample size of 0.25 grams.

After replacing the electrochemical sensors, the pure activated carbon and potassium hydroxide was tested again to reference the new sorbents being tested. Figure 13 shows the results that came from additional sorbents. These sorbents were Mn[EMIM][OAc], Zn[EMIM][OAc] 5% & 10%, Mg[EMIM][OAc], boric acid, pure activated carbon, and potassium hydroxide. These sorbents were again compared to industry standard potassium hydroxide and pure activated carbon to demonstrate improvement on sorption capabilities.

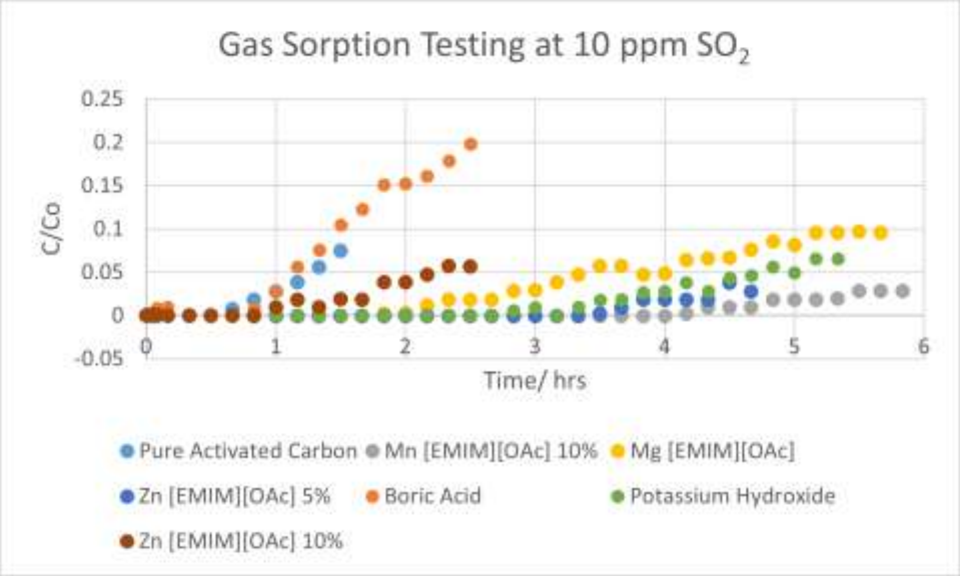

Figure 13: Impregnated activated carbon tested for 10 ppm SO_2 capture under realistic atmospheric conditions using a sample size of 0.25 grams with new sensors.

4.0 DISCUSSION

4.1 Incipient Impregnation Success/Non-Success

To successfully impregnate the sorbent onto the activated carbon, it was necessary to add a solvent to the sorbent for dissolution. In some cases, sorbents with high solubility dissolution were easily completed, but because such small amounts were used with small glassware, the solubility experiments were at many times difficult, especially because some sorbents were only soluble with solvents that had significantly high melting points which wouldn't allow extraction of the solvent out of the solution in the utilized method. Water and methanol were found to be the best solvents to use because of their high polarity and because they were easily removed using the vacuum oven. Water was also beneficial to use during these solubility experiments because if the sorbent's solubility was low, then heat was easily added without having safety issues.

4.2 Screening of Activated Carbon Size

Activated carbons are a suitable choice for acidic gas sorption because of their significant porosity and high surface area. Their potential for SO_2 sorption is presented in Figure 9 and indicates that activated carbon alone is capable of sorbing SO_2. The SO_2 sorption capability of activated carbon demanded that an optimal size would be chosen to be capable of evaluating impregnated sorbents potential without wasting substantial amounts of time and gas. In Figure 9 the five sizes of pure activated carbon are 0.2 g, 0.25 g, 0.3 g, 0.5 g, and 1.0 g.

The 1.0 g and the 0.5 g of activated carbon demonstrated substantially long sorption times with hardly any breakthrough. They both went 4 hours without any breakthrough, demonstrating and conveying that this size of samples for gas sorption testing was not optimal. If impregnated sorbents were effective, the experiments would have been capable of running past 6-7 hours without breaking through. Smaller samples were then tested to evaluate the breakthrough capacity times. The 0.2 g sample broke through immediately and the 0.3 g sample broke through at roughly 65-75 minutes. When testing the middle ground at 0.25 g of activated carbon, the ideal sample size was determined. This was because it broke through almost immediately similar to the 0.2 g sample, but the 0.25 g sample had more mass and was able to indicate the impregnated sorbents capabilities more clearly.

The 0.25 g sample data was isolated as shown in Figures 10 & 11, showing the breakthrough times for the pure activated carbon with the old sensors and the new sensors. The old electrochemical sensors had a much shorter breakthrough capacity compared to the new electrochemical sensors. This can be explained by the old electrochemical sensors being more saturated causing it to signal SO_2 on the outlet GSM-60 sensor more quickly then the new sensors. This is why when using the old sensors, the analysis was only looking at the trends of the data. The old sensors had a breakthrough time of 10 minutes and a gradual increase over 4 hours. The new sensors had an approximate breakthrough of 30-40 minutes with a gradual increase for the next hour. The experiment was stopped shortly after because only the breakthrough capacity was of concern to determine capabilities of the impregnated sorbents.

4.3 Gas Sorption Testing on Impregnated Activated Carbon

In Figure 12, the data displays the different sorbents that were initially screened for 10 ppm of SO_2 sorption. The different sorbents tested were pure activated carbon, melamine, tetramethylurea 30%, tetramethylurea 10%, potassium hydroxide, and urea. The pure activated carbon and potassium hydroxide were both proxies to identify if the sorbents were viable or not. They were used as proxies because they are both used in industrial practices for desulphurization, as well as desulphurization in fuel cell vehicles. The other sorbents were tested because in literature they have been proven to have some acidic gas capture capabilities, and this project meant to explore their capabilities using specific methods of impregnation and gas sorption. The impregnated potassium hydroxide in Figure 12 clearly indicates superior SO_2 sorption and all the newly impregnated sorbents broke through almost immediately. Most of the sorbents broke through even before the pure activated carbon, and it was assumed that their poor performance was due to the impregnated sorbent blocking the pores and not allowing any SO_2 interaction, as well as having poor kinetics and capabilities for SO_2 sorption. Therefore, it was determined that none of the newly tested sorbents had viable characteristics for SO_2 sorption and the project moved into testing metallo ionic liquids and any remaining sorbents that hadn't been tested.

In Figure 13, the plot displays the different sorbents tested. The list includes pure activated carbon, Zn[EMIM][OAc] 5%, Zn[EMIM][OAc] 10%, Mn[EMIM][OAc], Mg[EMIM][OAc], boric acid, and potassium hydroxide. The potassium hydroxide and pure activated carbon were both used as frameworks for industry standards again. In this screening of impregnated sorbents, the sorbents had significantly improved SO_2 sorption.

Boric acid, being the last non metal ionic liquid sorbent that was tested, had similar breakthrough capacity of the non metallo ionic liquids with a breakthrough right after the pure activated carbon. The Zn[EMIM][OAc] 5% had a promising breakthrough time of roughly 3-1/2 hours and this surpassed the industry standards and presented efficient SO_2 sorption. In addition, it was explored if at higher concentrations of Zn[EMIM][OAc] the performance would be even better. This led to testing the Zn[EMIM][OAc] at 10% weight concentration with unfortunately poor results. The Zn[EMIM][OAc] 10% broke through at roughly 1 hour and had a much shorter breakthrough capacity compared to the 5% version. It is again assumed that the higher weight concentration of the Zn[EMIM][OAc] had low performance because it may have had some blockages of the activated carbon pores due to the higher amounts of sorbent impregnated.

Other metallo ionic liquids that were evaluated for SO_2 sorption were Mn[EMIM][OAc] and Mg[EMIM][OAc]. The Mg[EMIM][OAc] showed some SO_2 sorption capabilities but had a shorter breakthrough capacity then potassium hydroxide. Lastly, Mn[EMIM][OAc] had the best results with a breakthrough capacity of approximately 4 hours. Manganese demonstrated the best SO_2 sorption results which could be credited to the acetate groups in the ionic liquids and the high kinetics associated to be able to have efficient SO_2 interactions and sorption.

The plots of Zn[EMIM][OAc] and Mn[EMIM][OAc] were then isolated and are displayed below in Figures 14 & 15. The plots display the long breakthrough capacities of the filter media compared to activated carbon. The plots also show integrals of leveling off after the breakthrough that indicated that the sorbents might present viable candidates for industry filter media because they would have substantially long periods until saturation capacity is met. This was tested with the Zn[EMIM][OAc] 5% to see how well the impregnated sorbent would do over a long period of gas sorption with lower concentrations. In Figure 16, Zn[EMIM][OAc] 5% was tested for approximately 22 hours with an SO_2 concentration of 5 ppm, with subsequent experimental conditions as others to be able to see what the capabilities of these newly created filter media had. Figure 16 indicates that in lower acidic gas concentrations the filter media had even better results and stayed consistent with those results for a long period of time. After 22 hours the concentration on the outlet sensor was only 0.4 ppm of SO_2 indicating that lower concentrations allowed the kinetics of the sorbent to transpire more efficiently.

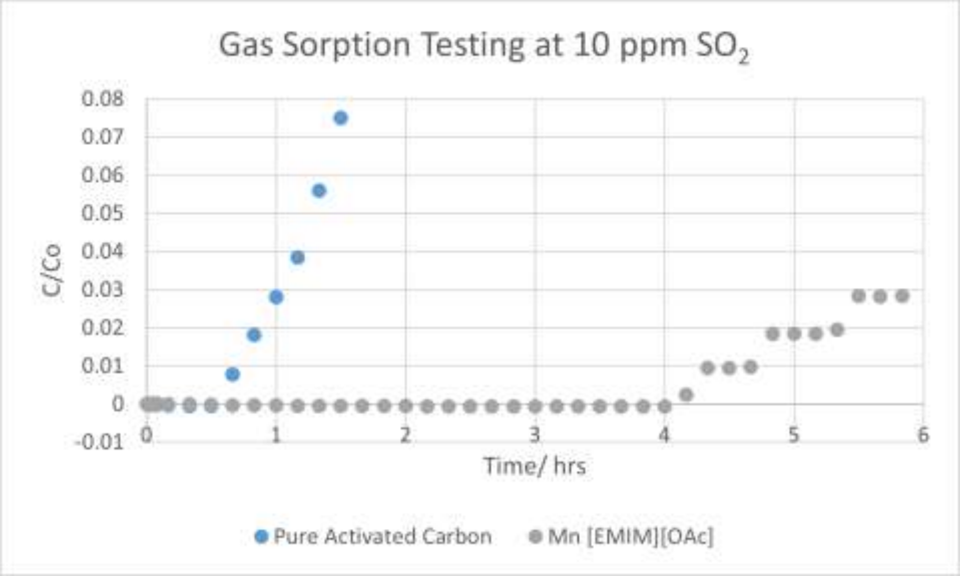

Figure 14: Mn[EMIM][OAc] Impregnated activated carbon tested for 10 ppm SO_2 capture under realistic atmospheric conditions using a sample size of 0.25 grams with new sensors.

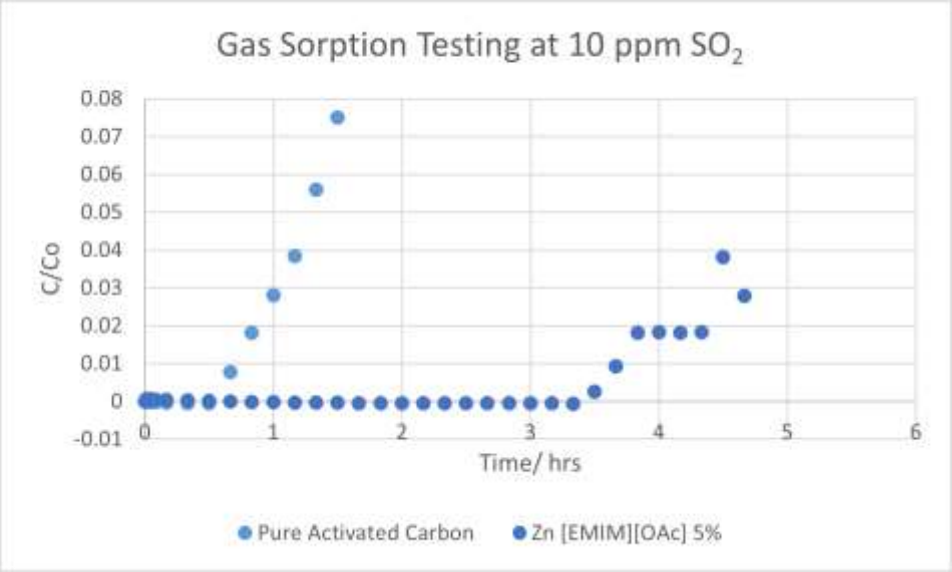

Figure 15: Zn[EMIM][OAc] Impregnated activated carbon tested for 10 ppm SO_2 capture under realistic atmospheric conditions using a sample size of 0.25 grams with new sensors.

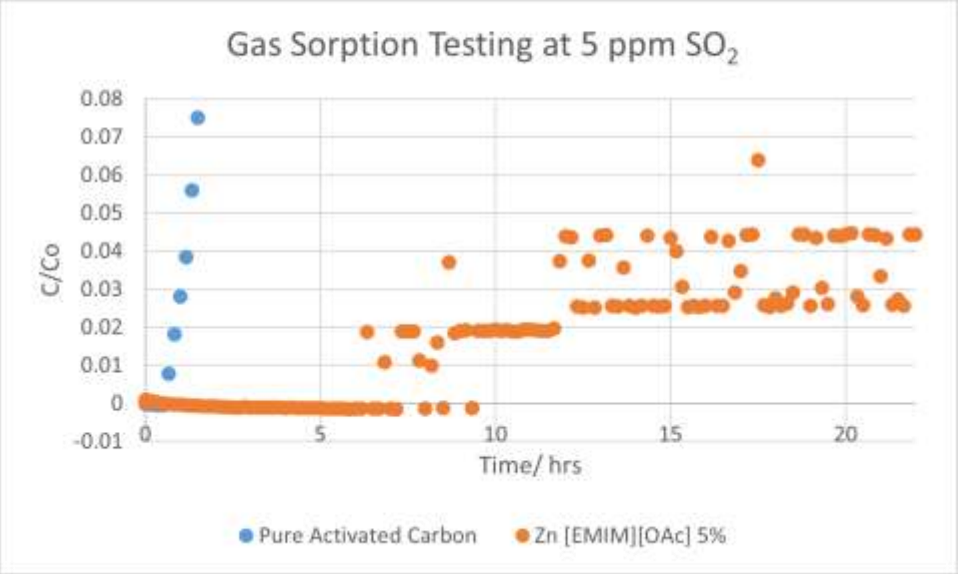

Figure 16: Zn[EMIM][OAc] Impregnated activated carbon tested for 5 ppm SO_2 capture under realistic atmospheric conditions using a sample size of 0.25 grams with new sensors.

5.0 CONCLUSION

After incipient impregnation was completed, the sorbents were successfully impregnated onto the activated carbon at different weight concentrations. After multiple gas sorption screenings, SO_2 sorbed onto the newly created sorbents under experimental conditions resulting in new sorbents being found for gas capture of SO_2.

The new sorbents that found most success with SO_2 capture were the metallo ionic liquids, specifically the 10% Mn[EMIM][OAc] and 5% Zn [EMIM][OAc]. The success in metal ionic liquids impregnated onto activated carbons can be credited to the high surface area and high porosity of activated carbon which allowed impregnation of thin films of metallo ionic liquids for effective reaction with the SO_2. Success came from higher reaction kinetics of metallo ionic liquids and SO_2.

Further actions that can be taken are completing characterization of the sorbed filter media as well as changing the conditions of the filter media. Fourier transform infrared spectroscopy could be utilized to be able to detect if any SO_2 effectively sorbed to the filter media. Thermogravimetric analysis would be able to identify what the exact weight concentrations of sorbents impregnated onto the activated carbon is. Other further actions could be testing the filter media at other relative humidity's, different flow rates, different temperatures, different acidic gases (e.g., H_2S, NO_2, CO_2), different impurity concentrations, and mixed impurities.

APPENDIX.

Steps	Procedure
1	Pour unwashed activated carbon into appropriate beaker
2	Fill the beaker with sink water and stir activated carbon with long stirring tool
3	The water was drained out of beaker using a cloth filter to capture the activated carbon
4	The captured activated carbon was then placed back into beaker and the process was repeated approximately 5-6 times using sink water, then an additional 5-6 times using deionized water
5	Activated carbon sat on cloth filter for approximately 1 hour, and then placed into vacuum oven and dried at 105˚C for 48 hours

Appendix 1.

Steps	Procedure
1	Dissolution of sorbent and solvent in a 5 mL volumetric flask
2	Once fully dissolved, extract appropriate amount of solution and pipet into 125 mL flask
3	Add the activated carbon onto the solution in the 125 mL flask, and take to the vortex mixer for agitation
4	Agitate on vortex mixer for 5 seconds on and 5 seconds off at 1500 rpm, after doing this for 4-5 times increase intervals of agitation up to 10 seconds on and 10 seconds off, and then decrease back to the 5 seconds interval
5	Sample sits for 20 hours at 25 ˚C and then is dried in a vacuum oven for 5 hours at 105 ˚C, and then taken out and stored in an inert glovebox

Appendix 2.

Steps	Procedure
1	Set all filtrations stand conditions (flow rates, humidifier, dewpoint), bypass reactor flowing gas mixture only to inlet and outlet sensors
2	Place sample into the reactor and measure the length of the sample
3	Direct the flow rates to the reactor and record the start time, to reference when extracting data
4	Once breakthrough capacity is reached, set flows to bypass the reactor and flush the system with clean air for 15 minutes to remove acidic gases from the pipes.
5	Remove the sample from reactor and store wrapped in para film. Then stop flow rates, turn off humidifier and extract data from software.

Appendix 3.

LITERATURE CITED

Aguilar-Dodier, L. C., Castillo, J. E., Quintana, P. J. E., Montoya, L. D., Molina, L. T., Zavala, M., Almanza-Veloz, V., & Rodríguez-Ventura, J. G. (2020). Spatial and temporal evaluation of H2S, SO2 and NH3 concentrations near Cerro Prieto geothermal power plant in Mexico. *Atmospheric Pollution Research*, *11*(1), 94–104.

Bandosz, T. J. (1999). Effect of pore structure and surface chemistry of virgin activated carbons on removal of hydrogen sulfide. Carbon, 37(3), 483–491.

Colella, W. G., Jacobson, M. Z., & Golden, D. M. (2005). Switching to a U.S. hydrogen fuel cell vehicle fleet: The resultant change in emissions, energy use, and greenhouse gases. *Journal of Power Sources*, *150*(1), 150–181.

Cheng, X., Shi, Z., Glass, N., Zhang, L., Zhang, J., Song, D., Liu, Z.-S., Wang, H., & Shen, J. (2007). A review of PEM hydrogen fuel cell contamination: Impacts, mechanisms, and mitigation. *Journal of Power Sources*, *165*(2), 739–756.

Dera, Bruffey, E., Finkelstein, G. J., Kelly, C., Gigante, A., Hagemann, H., & Severa, G. (2020). Synthesis, Characterization, and Crystal Structures of Two New Manganese Aceto EMIM Ionic Compounds with Chains of Mn2+ Ions Coordinated Exclusively by Acetate. ACS Omega, 5(25), 15592–15600

EPA. (2021). Carbon Pollution from Transportation. EPA. Retrieved from https://www.epa.gov/transportation-air-pollution-and-climate-change/carbon-pollution-transportation.

Eufrasio, R. M., Kantzas, E. P., Edwards, N. R., Holden, P. B., Pollitt, H., Mercure, J.-F., Koh, S. C. L., & Beerling, D. J. (2022). Environmental and health impacts of atmospheric CO2 removal by enhanced rock weathering depend on nations' energy mix. *Communications Earth & Environment*, *3*(1), 1–13.

Freudenberg. (2021). Freudenberg Fuel Cell Components. Freudenberg Fuel Cell Components - Freudenberg Performance Materials. Retrieved from https://fuelcellcomponents.freudenberg-pm.com/en.

Georgiadis, A., Charisiou, N., & Goula, M. (2020). Removal of hydrogen sulfide from various industrial gases: A review of the most promising adsorbing materials. Catalyst, 10(5).

Grennfelt, P., Engleryd, A., Forsius, M., Hov, Ø., Rodhe, H., & Cowling, E. (2020). Acid rain and air pollution: 50 years of progress in environmental science and policy. *Ambio*, *49*(4), 849–864.

Haile, S. M. (2003). Materials for fuel cells. ScienceDirect, 6(3).

He, X., Wang, F., Wallington, T. J., Shen, W., Melaina, M. W., Kim, H. C., De Kleine, R., Lin, T., Zhang, S., Keoleian, G. A., Lu, X., & Wu, Y. (2021). Well-to-wheels emissions, costs, and feedstock potentials for light-duty hydrogen fuel cell vehicles in China in 2017 and 2030. Renewable and Sustainable Energy Reviews, 137, 110477.

Institute of Clean Air Companies. (2016). DRY SORBENT INJECTION FOR ACID GAS CONTROL: PROCESS CHEMISTRY, WASTE DISPOSAL AND PLANT OPERATIONAL IMPACTS. Arlington, Virginia; Institute of Clean Air Companies.

Jiang, X.-Q., Mei, X.-D., & Feng, D. (2016). Air Pollution and Chronic Airway Diseases: What Should People Know and Do?

Kazemi Shariat Panahi, H., Dehhaghi, M., Kinder, J. E., & Ezeji, T. C. (2019). A review on green liquid fuels for the transportation sector: a prospect of microbial solutions to climate change. *Biofuel Research Journal*, *6*(3), 995–1024.

Lv, H., Shen, Y., Xu, X., Zhou, W., Yang, D., & Zhang, C. (2022). Structure simulation design of a cathode air filter for SO2 contamination on a 7 kW fuel cell sightseeing vehicle. *International Journal of Hydrogen Energy*, *47*(8), 5521–5530.

Manisalidis, I., Stavropoulou, E., Stavropoulos, A., & Bezirtzoglou, E. (2020). Environmental and health impacts of Air Pollution: A Review. Frontiers in Public Health, 8.

Office of Energy Efficiency & Renewable Energy. (2020, May 5). Challenges. www.fueleconomy.gov - the official government source for fuel economy information. Retrieved from https://www.fueleconomy.gov/feg/fcv_challenges.shtml.

Severa, G., Bethune, K., Rocheleau, R., & Higgins, S. (2015). SO2 sorption by activated carbon supported ionic liquids under simulated atmospheric conditions. Chemical Engineering Journal, 265, 249–258.

Severa, G., Head, J., Bethune, K., Higgins, S., & Fujise, A. (2018). Comparative studies of Low Concentration SO2 and NO2 sorption by activated carbon supported [C2MIM][AC] and Koh Sorbents. Journal of Environmental Chemical Engineering, 6(1), 718–727.

Stephens, G. L., Wild, M., Stackhouse, P. W., L'Ecuyer, T., Kato, S., & Henderson, D. S. (2012). The Global Character of the Flux of Downward Longwave Radiation. *Journal of Climate*, *25*(7), 2329–2340.

Qiao, H., Zheng, F., Jiang, H., & Dong, K. (2019). The greenhouse effect of the agriculture-economic growth-renewable energy nexus: Evidence from G20 countries. *The Science of the Total Environment*, *671*, 722–731.